Science of Sintering, **51** (2019) 71-79

doi: https://doi.org/10.2298/SOS1901071M

UDK 549.73; 676.017.5; 532.74

Combined Magnetic and Structural Characterization of Hidrothermal Bismuth Ferrite ($BiFeO_3$) Nanoparticles

Jelena Maletaškić[1,2*)], Maria Čebela[1], Marija Pekajski Đorđević[1], Denis Kozlenko[3], Sergey Kichanov[3], Miodrag Mitrić[4], Branko Matović[1]

[1]Centre of Excellence-CextremeLab Vinca, Materials Science Laboratory, Institute of Nuclear Sciences, Vinča, University of Belgrade, Mike Petrovica Alasa 12-14, 11000 Belgrade, Serbia

[2]Laboratory for Advanced Nuclear Energy, Institute of Inovative Research, Tokyo Institute of Technology, 2-12-1, Ookayama, Meguro-ku, Tokyo, 152-8550 Japan

[3]Frank Laboratory of Neutron Physics, Joint Institute for Nuclear Research, Dubna, Russia

[4]Vinča Institute of Nuclear Sciences, University of Belgrade, Laboratory for Theoretical and Condensed Matter Physics, 11001, Belgrade, Serbia

Abstract:

Bismuth ferrite ($BiFeO_3$) was synthesized by hydrothermal method. The crystal and magnetic structures of $BiFeO_3$ have been studied by means of X-ray diffraction and neutron powder diffraction at ambient temperature. Microstructure was analysed by scanning electron microscopy. Quantitative phase analysis by the Rietveld method was conducted and crystallite sizes of 27 nm were determined from the XRD line broadening. The magnetic structure of $BiFeO_3$ is described by the G-type antiferromagnetic order with magnetic peak located at 4.6 Å and a noticeable magnetic contribution to a reflection located at 2.4 Å in the diffraction pattern. The values of the ordered magnetic moment of Fe ions μFe=3.8(1) μB, obtained at ambient conditions, are consistent with those determined earlier. The magnetic moments in the crystal plane z = const are arranged in parallel, changing the direction from [100] to [$\overline{1}10$] when moving from one to the other z = const plane.

***Keywords**: Bismuth ferrite; Magnetic structures; Neutron powder diffraction.*

1. Introduction

The multiferroic materials, exhibiting simultaneously ferroelectric and magnetic orders, recently have become a subject of extensive scientific research. Magnetoelectric multiferroic materials exhibit magnetic and ferroelectric order in the same temperature range, and they potentially offer a range of new applications, including spintronics, new data-storage media, and multiple-state memories [1-3]. Bismuth ferrite ($BiFeO_3$) has recently drawn attention due to its outstanding multi-functional properties, as well as the lead-free material**.** Bismuth ferrite ($BiFeO_3$) is one of the most researched single-phase multiferroic materials. A number of studies have been focused on this compound, motivated by its multiferroic properties and the potentially high magnetoelectric property. Single phase $BiFeO_3$ has received special attention due to its ferroelectric transition temperature of 1100 K and an antiferromagnetic Neel temperature up to 640 K [4, 5]. The coexistence of ferroelectric and

*) **Corresponding author:** jelena.pantic@vinca.rs

antiferromagnetic orders makes this material one of the most promising candidates for magnetoelectric applications at room temperature. It has also been established that residual porosity location, microstructure, size, grain growth habit and grain boundary geometry of the sintered specimen are very important factors to determine the electrical and magnetic properties of $BiFeO_3$.

Research on the multiferroic materials in recent years has greatly benefited from new developments and advanced methodology in the characterization processing pathways. The preparation of pure $BiFeO_3$ is often demanding and quite complicated because of the narrow interval of its thermal stability and the formation of secondary phases $Bi_{25}FeO_{40}$ and $Bi_2Fe_4O_9$ [6, 7]. Namely, according to the phase diagram of Bi_2O_3–Fe_2O_3, BFO is an incongruently melting compound [8, 9] and the kinetics of phase formation in the Bi_2O_3–Fe_2O_3 system can easily lead to the appearance of impurities such as $Bi_{25}FeO_{40}$, $Bi_2Fe_4O_9$ and Bi_2O_3 when prepared by solid state reaction route [6, 7]. It is also reported [7, 8] that successful synthesis of single phase of $BiFeO_3$ essentially may be dependent on the purity (99.9995 %) of the starting materials. To overcome these issues other methods have been developed such as ferrioxalate precursor method, sol–gel process, co-precipitation, spark plasma sintering and hydrothermal method [9-16]. Hydrothermal synthesis offers many advantages over conventional and non-conventional synthesis methods. The costs of instrumentation, energy and precursors for hydrothermal method are very low many comparing to advanced methods. In the present work we studied in detail the crystal and magnetic structure of $BiFeO_3$ nano-powders synthesized by the hydro-thermally route under strictly controlled temperature conditions. The unique pressure-temperature interaction of the hydrothermal solution allows us to prepare $BiFeO_3$ phase that is difficult to prepare with other synthetic methods.

2. Materials and Experimental Procedures

2.1. Synthesis procedure

In this work the chemical regents used were bismuth nitrate [$Bi(NO_3)_3{\cdot}5H_2O$], iron nitrate [$Fe(NO_3)_3{\cdot}9H_2O$] and potassium hydroxide (KOH). All the chemicals were analytical grade purity and were used as received without further purification. In this paper, the procedure proposed by the Han [16] was applied and it is described in details in previous work [18].

The equimolar mixtures of $Bi(NO_3)_3{\cdot}5H_2O$ and $Fe(NO_3)_3{\cdot}9H_2O$ were dissolved in 40 ml of KOH. The molar ratio of the alkali mineralizer was adjusted by dissolving certain amounts of KOH pellets into the distilled water.

The mixture was under constant magnetic stirring for 30 min and transferred into the autoclave. The autoclave was sealed, heated up to 200 ^oC and held for 6 hours, and then cooled to the room temperature naturally.

The produced powders were collected at the bottom of the Teflon liner after cooling to the room temperature. The products were washed at least five times by the repeated cycles of centrifugation in distilled water, and re-dispersed in ethanol by sonicating for 45 min. Subsequently, the actual powders were obtained by evaporating ethanol in a mortar heated at the temperature of 60 ^oC.

2.2. Characterization techniques

Neutron powder diffraction measurements were performed with the DN-12 spectrometer [19] at the IBR-2 high-flux pulsed reactor (FLNP JINR, Dubna, Russia). Diffraction patterns were collected at scattering angles $2\theta = 90°$. The spectrometer resolution at $\lambda = 2$ Å is $\Delta d/d = 0.012$ for this angle. The typical data collection time at one temperature

was 1 h. The sample volume was about 50 mm^3. The neutron diffraction data were analyses by the Rietveld method using FULLPROF program [20].

Sample was also characterized at room temperature by X-ray powder diffraction (XRPD) using Ultima IV Rigaku diffractometer, equipped with Cu $K_{\alpha1,2}$ radiation, using a generator voltage (40.0 kV) and a generator current (40.0 mA). The range of 20 - 80° 2θ was used for all powders in a continuous scan mode with a scanning step size of 0.02° and at a scan rate of 1°/min. Phase analysis was done by using the PDXL2 software (version 2.0.3.0) [20], with reference to the patterns of the International Centre for Diffraction Data database (ICDD) [21], version 2012. The investigated structures were visualized by using VESTA [22] software.

Scanning electron microscopy (SEM) was employed for the characterization of the crystallite morphology. The structure of the sample was characterized by a Tescan MIRA3 field emission gun scanning electron microscope, at 10 kV in high vacuum. Sample preparation for SEM measurements was carried out as followed. The powder was sonicated in ethanol for 5 minutes. Immediately afterwards, a drop of solution was casted onto a freshly cleaved kish graphite crystal embedded with a silver paste into a sample holder. Access material was removed in a stream of argon gas. The sample was first annealed at 90 ^oC for 15 minutes in air, and afterwards left to be degassed in low vacuum for 30 minutes.

3. Results and Discussion

The detailed information on crystal and magnetic structure parameters of $BiFeO_3$ phase was obtained by means of neutron diffraction, which allows to determine coordinates of light oxygen atoms with much better accuracy in comparison with X-ray diffraction and can direct studies a magnetic structure of $BiFeO_3$. Sample was selected in order to refine their crystal and magnetic structure parameters using the Fullprof program [23-25], which allows refining the lattice parameters, atomic coordinates, magnetic moments and its directions simultaneously. All the structure models i.e. cif files for refinement are taken from American Mineralogist Crystal Data Structure Base (AMCDSB) [26]. $BiFeO_3$ crystallizes in rhombohedral cell (space group *R*3*c*) as a single phase. In this perovskite structure, atoms are located in these positions: Bi, Fe in 6a (0, 0, *z*), and O in 18b (*x*, *y*, *z*) [27]. Result of Rietveld structural refinement as the best fit between calculated and observed neutron diffraction pattern is shown in Fig. 1. Refined crystallographic parameters of studied sample with corresponding agreement factors are given in Table I.

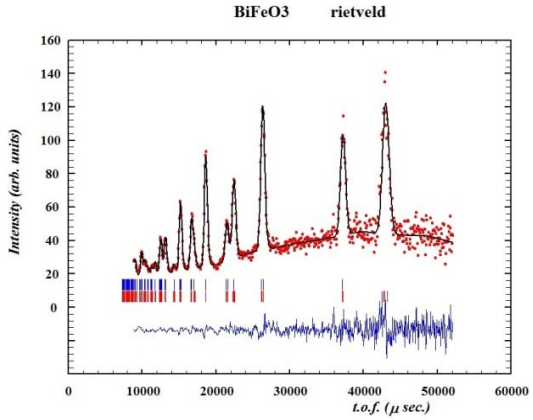

Fig. 1. Neutron diffraction patterns of $BiFeO_3$ measured at ambient temperature using the DN-12 detector banks located at scattering angles 2θ =90°. Tickmarks at the bottom represent the calculated positions of nuclear structure peaks of the ambient pressure rhombohedral phase (upper row) and the magnetic reflection (lower row).

Tab. I Refined structural parameters for $BiFeO_3$ and corresponding agreement factors.

Space group	***R3c***	***R3c***
	Neutron diffraction	*X-ray diffraction*
Cell parameters (Å)	a = 5.536(5)	a = 5.585(8)
	b = 5.536(5)	b = 5.585(8)
	c = 13.703(2) $\alpha = \beta$ = 90 °	c = 13.884(2) $\alpha = \beta$ = 90 °
	β = 120 °	β = 120 °
Vol(Å^3)	363.776(2)	375.080(9)
Goodness of refinement	R_{wp} = 3.05 R_p = 2.90	R_{wp} = 6.97 R_p = 5.53
	R_{mag} = 4.19	R_e = 6.37
	χ^2 = 1.8298	χ^2 = 1.1951

Table II and III shows fractional atomic parameters and magnetic moment projection of refined sample, while Table IV depicts selected interatomic distances. The distances Bi-O, Fe-O in space group *R*3*c* show good agreement with previously obtained data [28].

Tab. II Fractional atomic parameters with estimated standard deviation (in parentheses) for sample.

Element	**x**	**y**	**z**	**Occ**	**B (Å^2)**
Bi	0.00000(0)	0.00000(0)	0.00000(0)	1	0.2
Fe	0.00000(0)	0.00000(0)	0.22080(0)	1	0.5
O	0.44600(0)	0.01740(0)	0.95170(0)	3	1.0

Tab. III Fractional atomic parameters and projection of magnetic moments with estimated standard deviation (in parentheses) for sample.

Atoms	**x**	**y**	**z**	**Mx**	**My**	**Mz**	**Occ**	**B(Å^2)**
Fe 1	0.00000(0)	0.00000(0)	0.22080(0)	0.001(0)	5.376(146)	0.001(0)	1.000(0)	0.500
Fe 2	0.66667(0)	0.33333(0)	0.55416(0)	0.001(0)	5.376(146)	0.001(0)	1.000(0)	0.703
Fe 3	0.33333(0)	0.66667(0)	0.88749(0)	0.001(0)	5.376(146)	0.001(0)	1.000(0)	0.703
Fe 4	0.00000(0)	0.00000(0)	0.72082(0)	-5.376(146)	-5.376(146)	0.001(0)	1.000(0)	0.703
Fe 5	0.66667(0)	0.33333(0)	0.05416(0)	-5.376(146)	-5.376(146)	0.001(0)	1.000(0)	0.703
Fe 6	0.33333(0)	0.66667(0)	0.38749(0)	-5.376(146)	-5.376(146)	0.001(0)	1.000(0)	0.703

Tab. IV Selected interatomic distances nm (experimental data) with estimated standard deviation (in parentheses) for sample.

Bond	**Experimental values (nm)**
Bi – O	0.240(4)
Bi – O	0.243(4)
Fe – O	0.198(4)
Fe – O	0.204(5)

The magnetic structure of $BiFeO_3$ is described by the G-type antiferromagnetic order, which is indicated by the presence of a purely magnetic peak located at 4.6 Å and a noticeable magnetic contribution to a reflection located at 2.4 Å in the diffraction pattern (Fig. 1). The values of the ordered magnetic moment of Fe ions μ_{Fe} = 3.8(1) μ_B, obtained at ambient conditions, are consistent with those determined earlier. The arrangement of the magnetic moments of Fe ions is shown in Fig. 2. As can be seen from the Fig., the magnetic moments in the crystal plane z = const are arranged in parallel, changing the direction from *[100]* to [$\overline{110}$] when moving from one to the other z = const plane.

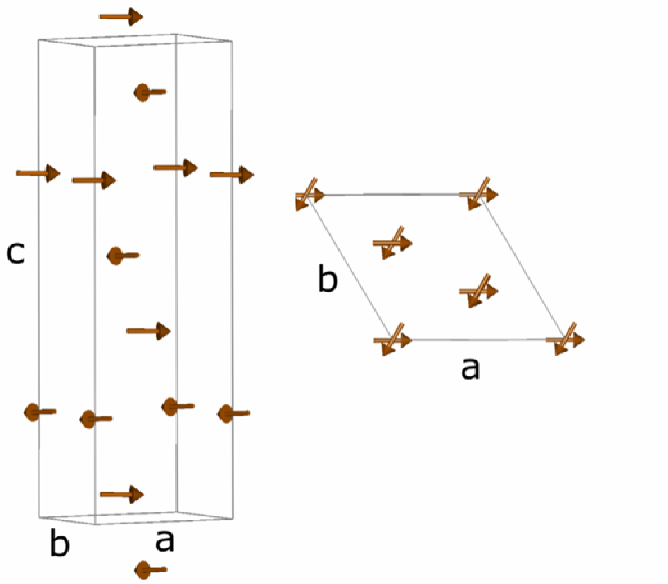

Fig. 2. The arrangement of the magnetic moments of Fe ions.

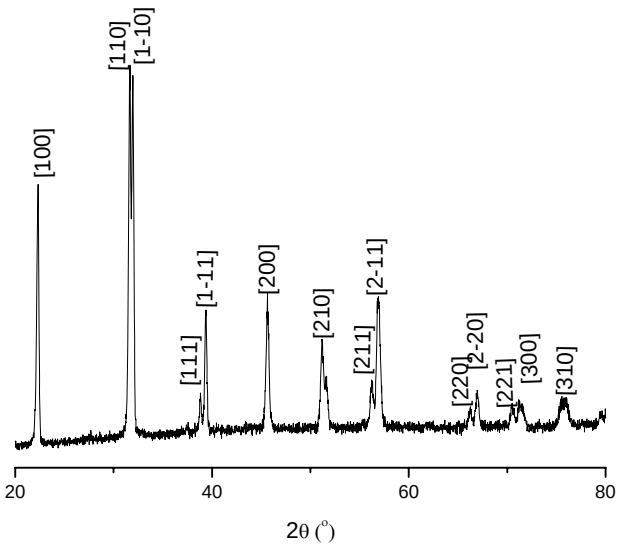

Fig. 3. XRD pattern of $BiFeO_3$ sample.

Fig. 3 presents XRD patterns of synthesized sample. The X-ray diffraction pattern shows Bragg peaks, which agree with the $BiFeO_3$ perovskite type of crystal structure described by the space group *R*3*c* [29-34]. Bismuth ferrite is a principle crystalline phase and

structural model found in literature (COD 2102909) [34] were used as starting structural model. Polyhedral net of the investigated samples is given in Fig. 4.

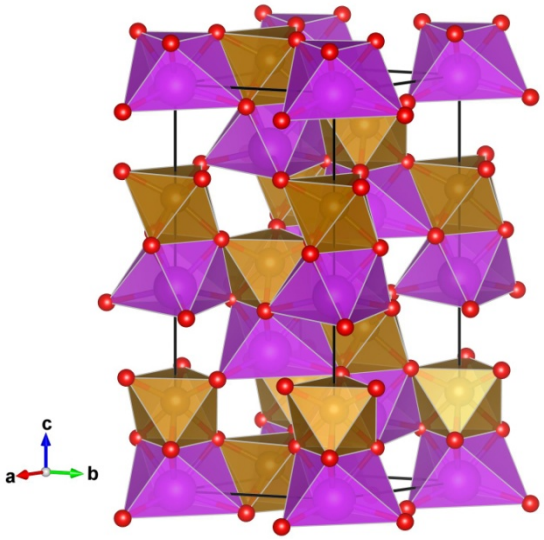

Fig. 4. Visualization of calculated structures of $BiFeO_3$ [19].

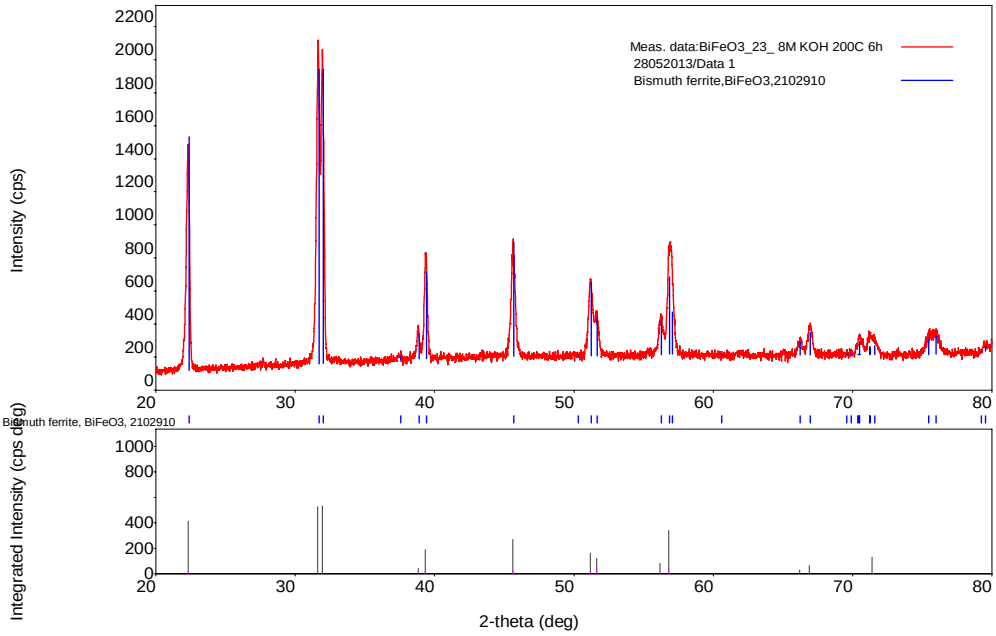

Fig. 5. Rietveld refinement plot of the X-ray powder diffraction data of the $BiFeO_3$.

Rietveld refinement method was carried on $BiFeO_3$ sample by using the PDXL2 software (version 2.0.3.0) [20], with reference to the patterns of the International Centre for Diffraction Data database (ICDD) [20], version 2012. Quantitative phase analysis by the Rietveld method was conducted using the Whole Pattern Fitting mode. We used the pseudo-Voigt peakshape and the background was interpolated between 14 points. Crystallite sizes were determined from the XRD line broadening using the Scherrer equation and the integral peak breadth (PDXL2 software). Obtained crystallite size of leading $BiFeO_3$ phase is 27 nm. Refined lattice parameters of $BiFeO_3$ of our sample, shown in Table I, are in good agreement

with the values found in the litterature [32]. Result of Rietveld structural refinement as the best fit between calculated and observed neutron diffraction pattern is shown in Fig. 5.

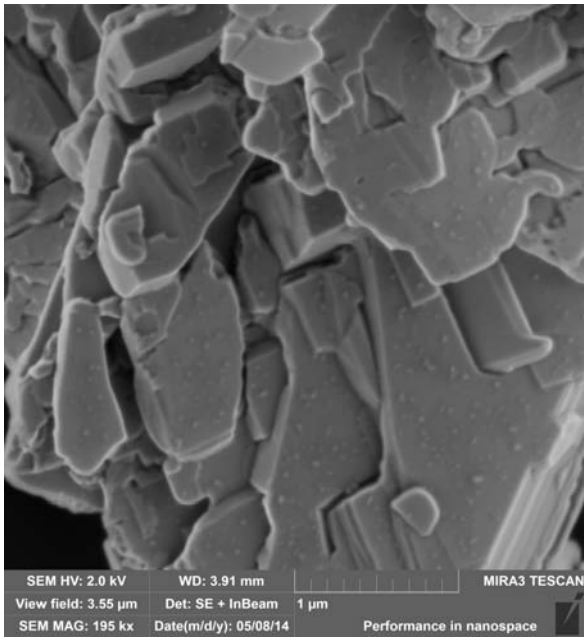

Fig. 6. SEM image of the crystallite morphology. Scale bar in the lower right corner corresponds to the length of 1 μm.

The result of SEM measurement that was performed at room temperature is shown in Fig. 6. SEM results reveal agglomeration of the matrix particles. $BiFeO_3$ shows plated morphology in layered structure. The plates are stacked tightly. The micrographs consist of irregularly shaped and stacked agglomerates that are larger than 1 μm in size. The average particle size estimated from XRPD data for $BiFeO_3$ is smaller than the average particle size that can be observed from SEM image, suggesting that the particles are composed of packed crystallites.

4. Conclusion

Pure phase $BiFeO_3$ was synthesized using hydrothermal method. Synthesis is done in sealed autoclave, heated at 200 ^oC and held for 6 hours. The magnetic structure of $BiFeO_3$ is refined with presence of a purely magnetic peak located at 4.6 Å. The values of the ordered magnetic moment of Fe ions μ_{Fe} = 3.8(1) μ_B are obtained at ambient conditions. Obtained crystallite size of leading $BiFeO_3$ phase is 27 nm. SEM results reveal agglomeration of the matrix particles and $BiFeO_3$ shows layered structure. As a room temperature multiferroic, $BiFeO_3$ has a potencial for the production being a lead free material.

Acknowledgments

This project was financially supported by the Ministry of Education and Science of Serbia (Project no. III 45012). This work has been enabled through the Russian-Serbian collaboration under the project with JINR, FLNP, Dubna, Russia.

5. References

1. Z. Ristanović, A. Kalezić – Glišović, N. Mitrović, S. Djukić, D. Kosanović, A. Maričić, Sci. Sinter. 47 (2015) 3.
2. S. L. Galagali, R. A. Patil, R. B. Adaki, C. S. Hiremath, S. N. Mathad, R. B. Pujar. Sci. Sinter. 50 (2018) 217.
3. E. A. Zereffa, T. A. Seghne, Sci. Sinter. 50 (2018) 245.
4. C. Michel, J. M. Moreau, G. D. Achenbach, R. Gerson, W. J. James, Solid State Comm. 7 (1969) 701.
5. J. R. Teague, R. Gerson, W. J. James, Solid State Comm. 8 (1970) 1073.
6. T. Lottermoser, T. Lonkai, U. Amann, D. Hohlwein, J. Ihringer, M. Fiebig, Nature 430 (2004) 541.
7. W. Eerenstein, N. D. Mathur, J. F. Scott, Nature 442 (2006) 759.
8. R. Ramesh, N. A. Spaldin, Nat. Mater. 6 (2007) 21.
9. S. Ghosh, S. Dasgupta, A. Sen, H.S. Maiti, Mater. Res. Bull. 40 (2005) 2073.
10. J. K. Kim, S. S. Kim, W.-J. Kim, Mater. Lett. 59 (2005) 4006.
11. H. Ke, W. Wang, Y. Wang, J. Xu, D. Jia, Z. Lu, Y. Zhou, J. Alloys Compd. 509 (2011) 2192.
12. T. P. Comyn, D.F. Kanguwe, J. He, A.P. Brown, J. Eur. Ceram. Soc. 28 (2008) 2233.
13. R. Mazumder, D. Chakravarty, D. Bhattacharya, A. Sen, Mater. Res. Bull. 44 (2009) 555.
14. X. Z. Chen, Z. C. Qiu, J. P. Zhou, G. Zhu, X. B. Bian, P. Liu, Mater. Chem. Phys. 126 (2011) 560.
15. B. Liu, B. Hu, Z. Du, Chem. Commun. 47 (2011) 8166.
16. A. Jaiswal, R. Das, K. Vivekanand, P. Mary Abraham, S. Adyanthaya, P. Poddar, J. Phys. Chem. C 114 (2010) 2108.
17. S. H. Han, K. S. Kim, H. G. Kim, H.-G. Lee, H.-W. Kang, J. S. Kim, C. I. Cheon, Ceram. Int. 36 (2010) 1365.
18. M. Čebela, D. Zagorac, K. Batalović, J. Radaković, B. Stojadinović, V. Spasojević, R. Hercigonja, Ceram. Int. 43 (2017) 1256.
19. A. Balagurov, Physica B 174 (1991) 542.
20. PDXL Version 2.0.3.0 Integrated X-ray Powder Diffraction Software. Tokyo, Japan: Rigaku Corporation; 2011, p. 196-8666.
21. Powder Diffraction File, PDF-2 Database and announcement of new database release 2012, International Centre for Diffraction Data (ICDD).
22. K. Momma, F. Izumi, J. Appl. Crystallogr. 41 (2008) 653.
23. J. Rodríguez-Carvajal, FullProf computer program, 1998, ftp://charybde.saclay.cea.fr/pub/divers/fullprof.98/windows/winfp98.zip.
24. J. Rodríguez-Carvajal, Recent developments of the program FULLPROF, in Commission on Powder Diffraction (IUCr). Newsletter 26 (2001) 12–9, http://journals.iucr.org/iucr-top/comm/cpd/Newsletters/.
25. J. Rodríguez-Carvajal, Physica B 192 (1993) 55.
26. R. T. Downs, M. Hall-Wallace, Am. Min. 88 (2003) 247.
27. F. Kubel, H. Schmid, Acta Cryst. B 46 (1990) 698.
28. J. M. Moreau, C. Michel, R. Gerson, W. J. James, J. Phys. Chem. Solids, 32 (1971) 1315.
29. P. Fischer, M. Połomska, I. Sosnowska, M. Szymański, J. Phys C 13 (1980) 1931.
30. A. Palewicz, R. Przeniosło, I. Sosnowska, A.W. Hewat, Acta Cryst. B 63 (2007) 537.
31. F. Kubel, H. Schmid, Acta Cryst. B 46 (1990) 698.
32. I. Sosnowska, W. Schäfer, W. Kockelmann, K. H. Andersen, I. O. Troyanchuk, Appl. Phys. A 74 (2002) 1040.
33. J. D. Bucci, B. K. Robertson, W. J. James, J. Appl. Cryst. 5 (1972) 187.
34. A. Palewicz, R. Przeniosło, Sosnowskaa, A. W. Hewat, Acta Cryst. B 63 (2007) 537.

Садржај: *Бизмут-ферит ($BiFeO_3$) је синтетисан користећи хидротермалну методу. Кристална и магнетна структура $BiFeO_3$ су утачњене помоћу рендгенске и неутронске дифракције праха на собној температури, користећи Ритвелдову методу. Микроструктура је анализирана помоћу скенирајуће електронске микроскопије. Квантитативном рендгенском анализом потврђено је присутво $BiFeO_3$ као главне и једине фазе, а величина кристалита од 27 nm одређена је анализом ширења дифракционих линија. Магнетна структура $BiFeO_3$ припада антиферомагнетним уређењу Г-типа, што је потврђено присутвом чистог магнетног пика који се налази на 4,6 Å, као и магнетским доприносом рефлексије смештеној на 2.4 Å на дифрактометру праха. Вредности магнетног момента Fe јона $\mu Fe = 3.8\ (1)\ \mu B$, добијене у амбијенталним условима, се поклапају са вредностима који су раније одређени. Магнетни моменти у кристалној равни z = const уређени су паралелно, наизменично мењајући правац од [100] до $[\overline{1}10]$ приликом преласка од једне до друге z = const равни.*

Кључне речи*: бизмут-ферит, магнетна структура, неутронска дифракције праха.*